Emergent Weyl fermion excitations in TaP explored by ^{181}Ta quadrupole resonance

H. Yasuoka,[1,2] T. Kubo,[1,3] Y. Kishimoto,[1,3] D. Kasinathan,[1] M. Schmidt,[1] B. Yan,[1] Y. Zhang,[1,4] H. Tou,[3] C. Felser,[1] A. P. Mackenzie,[1,5] and M. Baenitz[1,*]

[1] *Max Planck Institute for Chemical Physics of Solids, 01187 Dresden, Germany*
[2] *Advanced Science Research Center, Japan Atomic Energy Agency, Tokai, Ibaraki 319-1195, Japan*
[3] *Department of Physics, Graduate school of Science, Kobe University, 1-1 Rokkodai, Nada-ku, Kobe, 657-8501 Japan*
[4] *IFW Dresden, P.O. Box 270116, 01171 Dresden, Germany*
[5] *SUPA, School of Physics & Astronomy, University of St. Andrews, North Haugh, St. Andrews KY16 9SS, United Kingdom*

(Dated: November 23, 2016)

The ^{181}Ta quadrupole resonance (NQR) technique has been utilized to investigate the microscopic magnetic properties of the Weyl semi-metal TaP. We found three zero-field NQR signals associated with the transition between the quadrupole split levels for Ta with I=7/2 nuclear spin. A quadrupole coupling constant, $\nu_{\rm Q}$ =19.250 MHz, and an asymmetric parameter of the electric field gradient, η = 0.423 were extracted, in good agreement with band structure calculations. In order to examine the magnetic excitations, the temperature dependence of the spin lattice relaxation rate ($1/T_1T$) has been measured for the f_2-line ($\pm5/2 \leftrightarrow \pm3/2$ transition). We found that there exists two regimes with quite different relaxation processes. Above $T^* \approx 30$ K, a pronounced $(1/T_1T) \propto T^2$ behavior was found, which is attributed to the magnetic excitations at the Weyl nodes with temperature dependent orbital hyperfine coupling. Below T^*, the relaxation is mainly governed by Korringa process with $1/T_1T$ = constant, accompanied by an additional $T^{-1/2}$ type dependence to fit our experimental data. We show that Ta-NQR is a novel probe for the bulk Weyl fermions and their excitations.

PACS numbers: 02.40.Pc, 76.60.-k, 76.60.Gv, 31.30.Gs

The past decade has seen an explosion of interest in the role of topology in condensed matter physics. Major discoveries have included the two dimensional graphene[1] and the topological insulators (TI) (e.g. HgTe or Bi_2Se_3),[2–4] whose topological properties require the existence of gapless surface states. Many of the new materials host exotic excitations whose observation can be regarded as direct experimental evidence for the existence of quasiparticles. Arguably, the most topical of the new classes of materials are Dirac- and Weyl-semi metals which are predicted to host topologically protected states in the bulk.[5] In Dirac semimetals (DSM),[5–7] (e.g. Cd_2As_3 or Na_3Bi) each node contains fermions of two opposite chiralities, whereas in the Weyl semimetals (WSM),[8–12] an even more interesting situation arises. A combination of non-centrosymmetric crystal structure and sizable spin-orbit coupling (SOC) causes the nodes to split into pairs of opposite chirality (Weyl points). In the ideal case, there would be exactly half filling of the relevant bands, such that the Weyl points would sit at the Fermi level ($E_{\rm F}$) and the Weyl fermions would be massless. In actuality, Weyl semimetals such as the *d*-electron monophosphides NbP and TaP, $E_{\rm F}$ does not exactly coincide with the Weyl nodes.[9, 10, 12] However, if the nodes sit close enough to $E_{\rm F}$, in a region of linear dispersion ($E \propto k$), the Weyl physics can still be observed in the excitations in the energy window $k_{\rm B}T$. A key issue in the study of the monophosphides is therefore to establish how close to the Fermi level the Weyl points sit, and to estimate the range of energy over which the linear dispersion exists. This presents a considerable experimental challenge. The nodes appear in the electronic structure of the bulk, and the materials are fully three-dimensional, so the surface-sensitive techniques that have yielded immense insight into other topological physics are not ideally suited to studying the Weyl points. Primarily, one would like to identify a bulk probe that can excite the Weyl fermions and probe the linear dispersion $E \propto k$ indirectly via its energy dependence of the density of states around the Fermi level, which is $N(E) \propto E^2$ for a Weyl node.[5] The magnetic resonance method in general has the ability to probe $N(E)$, and was applied successfully to systems like unconventional superconductors (e.g. UPt_3)[13–16] or correlated magnetic semimetals[17] (e.g. SmB_6[18] or $CeRu_4Sn_6$[19]). In particular, for unconventional superconductors, the nuclear quadrupole resonance (NQR) spin lattice relaxation provides information about $N(E)$ around the $E_{\rm F}$ and allows us to distinguish between point nodes ($N(E) \propto E^2$) and line nodes ($N(E) \propto E$).[16] Therefore, NQR should be a good tool to study the low energy spin excitations in a Weyl semi metal and is the focus of our presented work. Assuming that some of the Weyl points are energetically not too far from $E_{\rm F}$, NQR can probe the magnetic excitations of emergent Weyl fermions via the temperature dependence of the spin-lattice relaxation rate ($1/{\rm T}_1T$). Furthermore, a characteristic temperature dependence of the hyperfine cou-

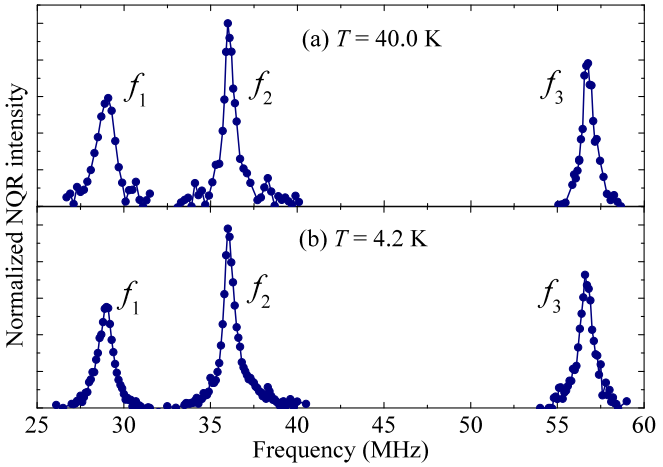

FIG. 1. Typical ^{181}Ta NQR spectra in TaP obtained from the spin-echo real part integration at 40 K (a) and 4.2 K (b). The data was taken in 0.1 MHz steps across the spectrum. The lines f_1, f_2 and f_3 correspond to $\pm 3/2 \leftrightarrow \pm 1/2$, $\pm 5/2 \leftrightarrow \pm 3/2$ and $\pm 7/2 \leftrightarrow \pm 5/2$ transitions, respectively.

pling between the nuclear spin and electric orbitals near the Weyl nodes has theoretically been predicted which modifies the temperature dependence of $(1/\mathrm{T}_1T)$ in a special manner.[20] In fact, TaP has been known to have two sets of Weyl nodes, one located 41 meV (476 K) below E_F and the other is located 13 meV (151 K) above E_F.[12] Accordingly, for temperatures coinciding with the Weyl nodes, excitations associated with the Weyl fermions are expected. Here, we present such characteristic excitations via Ta NQR experiments and explore the emergent Weyl fermion excitations in TaP.

Samples used in the present NQR study were prepared by the chemical transport method. In a first step, TaP was synthesized by direct reaction of the elements tantalum (Alfa Aesar 99.98%) and red phosphorus (Alfa Aesar 99.999%) at 500 °C and 600 °C in an evacuated fused silica tube for 72 hours. Starting from this microcrystalline powder, TaP was crystallized by a chemical transport reaction (CTR) in a temperature gradient from 900 °C (source) to 1000 °C (sink), and a transport agent concentration of 13 mg/cm^3 iodine (Alfa Aesar 99.998%). Crystals obtained by the CTR method were characterized by electron-probe-microanalysis and powder X-ray diffraction.

The NQR experiments were carried out with either a high quality single crystal or powder prepared from single crystals. The NQR spectra and $1/T_1T$ were measured using standard pulsed NMR (nuclear magnetic resonance) apparatus. The spectra were taken using the frequency sweep method under zero applied magnetic field. In order to avoid any artificial broadening, fast Fourier transformed (FFT) signals were summed across the spectrum (FFT-summation) or the real part was integrated after proper phase adjustment. Since T_1 is extremely long in TaP (typically several hundred seconds at low temperatures), we employed the progressive saturation method to measure the temperature dependence of $1/T_1T$.[21] The recovery of nuclear magnetization was fitted to the theoretical function[22] for the magnetic relaxation in NQR lines,

$$M_n(t) = M_0\left[1 - \left(Q_1 e^{(-K_1 t/T_1)} + Q_2 e^{(-K_2 t/T_1)} + Q_3 e^{(-K_3 t/T_1)}\right)\right] \quad (1)$$

where, Q_n and K_n are constants depending on which NQR transition is excited and the asymmetry parameter of the electric field gradient (EFG). Using a set of principal axes, the quadrupole Hamiltonian can be written as,[23]

$$H_Q = \frac{e^2qQ}{4I(2I-1)}\left[3I_z^2 - I(I+1) + \frac{1}{2}\eta(I_+^2 - I_-^2)\right] \quad (2)$$

where, eq is the largest component of the EFG tensor, V_{zz}, and eQ is the nuclear quadrupole moment. The EFG tensor is generally defined as $|V_{zz}| \geq |V_{yy}| \geq |V_{xx}|$, with the asymmetry parameter $\eta = (V_{xx} - V_{yy})/V_{zz}$. The quadrupole-split nuclear energy levels E_m, and the resultant transition frequencies can be readily calculated numerically by diagonalizing Eq. (2). For $\eta = 0$, the energy levels can simply be expressed as,

$$E_m = \frac{1}{6}h\nu_Q\left[3m^2 - I(I+1)\right], \nu_Q = \frac{3e^2qQ}{h2I(I-1)} \quad (3)$$

where ν_Q is the quadrupole coupling constant. The NQR occurs for the transition between two levels m and m+1 and the resonance condition can be written as $f_\mathrm{Q} = \nu_\mathrm{Q}(2|m|+1)/2$. Therefore, for $\eta = 0$, three NQR lines for I=7/2 are expected at ν_Q, $2\nu_\mathrm{Q}$ and $3\nu_\mathrm{Q}$ with equal spacing.

We searched for the NQR signal in TaP powder in a frequency range from 20 MHz to 80 MHz at 4.2 K and found three resonance lines. The observed ^{181}Ta NQR spectra at 4.2 K and 40 K are shown in Fig.1 (a) and (b). One can immediately observe that the three lines are not equally spaced, meaning that the value of η is sizable. By fitting each line at 4.2 K to a Lorentzian, we obtained the peak frequencies f_1 = 28.95 MHz, f_2 = 36.08 MHz and f_3 = 56.67 MHz. Although the full width at half maximum (FWHM) of the spectra is about 800 KHz, the line profiles are Lorentzian with long spectral tails. This implies that the EFG has a rather broad distribution. Since the Ta nuclear quadrupole moment is quite large (besides rare-earth and actinide elements, the ^{181}Ta nucleus has the second largest Q-value), the NQR spectrum can be broadened easily by merely a slight local inhomogeneity or nonstoichiometry in the composition. A least squares fit of the observed peak frequency to the theoretical quadrupole interaction obtained from exact diagonalization gives us ν_Q = 19.250 MHz and η = 0.423.

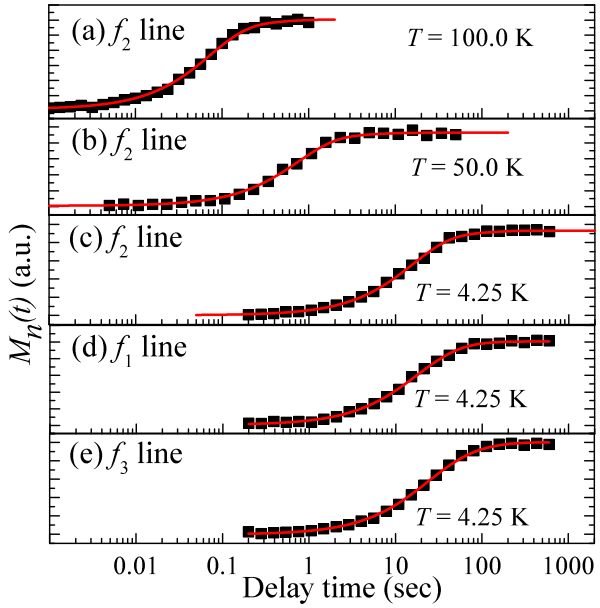

FIG. 2. (Color Online) Recovery of the nuclear magnetization M_n(t) measured by the NQR intensity after saturation to thermal equilibrium value for f_2 line at 100 K (a), 50 K (b), 4.25 K (c), f_1 line at 4.25 K (d) and f_3 line at 4.25 K (e). The red curves are the least squares fit of the data derived using Eq. (1). The perfect fit in all cases demonstrates the fact that the relaxation is governed by magnetic fluctuations.

$K_1 = 3.01028$, $K_2 = 8.7084$, $K_3 = 17.42483$			
f_1-line	$Q_1 = 0.05073$	$Q_2 = 0.45677$	$Q_3 = 0.49250$
f_2-line	$Q_1 = 0.07624$	$Q_2 = 0.02126$	$Q_3 = 0.90250$
f_3-line	$Q_1 = 0.19320$	$Q_2 = 0.51185$	$Q_3 = 0.29495$

TABLE I. The calculated pre-factors and exponents in Eq. (1) for $\eta = 0.423$, used for the least squares fit shown in Fig. 2.

The same results were also obtained for a small single crystal at 4.2 K. We also measured the spectra up to 80 K and found that there is no appreciable temperature dependence of the η value but ν_Q has a gradual decrease with increasing temperature (see Supplement for more details).

In order to extract the quadrupole interaction in TaP theoretically, we performed band structure calculations using the density functional theory (DFT) code FPLO.[24] We used the Perdew-Wang parametrization of the local density approximation (LDA) for the exchange-correlation functional.[25] The strong SOC in TaP is taken into account by performing full-relativistic calculations, wherein the Dirac Hamiltonian with a general potential is solved. The treatment of a finite nucleus is implemented in the code, necessary for accurate estimation of NQR parameters.[26] As a basis set, we chose Ta ($4f/5s5p6s7s8s5d6d7d6p7p5f$) and P ($2s2p3s4s5s3p4p5p3d4d4f$) semi-core/valence states. The higher lying states of the basis set are essentially important for the calculation of the EFG tensor with components $V_{ij} = \partial V/\partial x_i \partial x_j$. The low lying states were treated fully relativistically as core states. A well-converged k mesh in 1210 k-points was used in the irreducible part of the Brillouin zone. Theoretically, the quadrupole coupling, ν_Q can be obtained by calculating the electric field gradient (EFG) at the Ta nuclear site which is defined as the second partial derivative of the electrostatic potential v(r) at the position of the nucleus V_{ij} = ($\partial i \partial j$v(0) - $\Delta\delta_{ij}$v(0)/3). Our calculations result in V_{xx} = -1.186×10^{21} V/m^2, V_{yy} = -2.354×10^{21} V/m^2 and V_{zz} = 3.540×10^{21} V/m^2, where the principal axis of the EFG is [100] for one Ta atom and [010] for the second Ta atom in the unit cell. Using these values and Eq. (2) we obtained ν_Q = 20.057 MHz and η = 0.33. These theoretical values are in good agreement with the experimental values, assuring that our line assignment to the quadrupole transitions is correct.

Before discussing the temperature dependence of $1/T_1T$, we have to make sure that the relaxation is governed by the magnetic fluctuations associated with the conduction electrons, although the density is quite small in semi-metals. To answer this, we have made careful measurements of the time dependence of the recovery of nuclear magnetization from saturation to thermal equilibrium for all temperatures and NQR lines. Then, assuming that magnetic fluctuations are responsible for the nuclear relaxation process, the relaxation curves were fitted to Eq. (1) using calculated prefactors and exponents (Table. I) for the observed value of $\eta = 0.423$. The experimental results and fitted curves are shown in Fig. 2. Here, we have a perfect match between the two for all temperatures and NQR lines, providing very strong evidence that the relaxation process is totally governed by magnetic fluctuations and yielding assurance to the accuracy of the T_1 values that were extracted.

The temperature dependence of $1/T_1T$ has been measured mainly for the f_2-line and the obtained result is shown in Fig. 3(a). One can immediately observe that there exists a characteristic temperature $T^* \approx 30$ K, where the relaxation process has a crossover from a high temperature T^2 behavior (which is presumably associated with the excitations in the nodal structure of Weyl points) to the low temperature Korringa excitations[27] for parabolic bands ($E \propto k^2$ and $N(E) \propto \sqrt{E}$) with a weak temperature dependence.

Quite generally, $1/T_1T$ can be expressed using the wave vector (q) and frequency (ω) dependent magnetic susceptibility $\chi(q,\omega)$, characterizing the magnetic excitations in a system as,[28]

$$\frac{1}{T_1T} = \frac{2\gamma_n^2 k_B}{g^2\mu_B^2} \sum_q A_q^2 \frac{\chi''_\perp(q,\omega)}{\omega_n} \qquad (4)$$

where $\chi''_\perp(q,\omega)$ is the transverse component of imaginary part of $\chi(q,\omega)$, γ_n is the nuclear gyromagnetic ratio

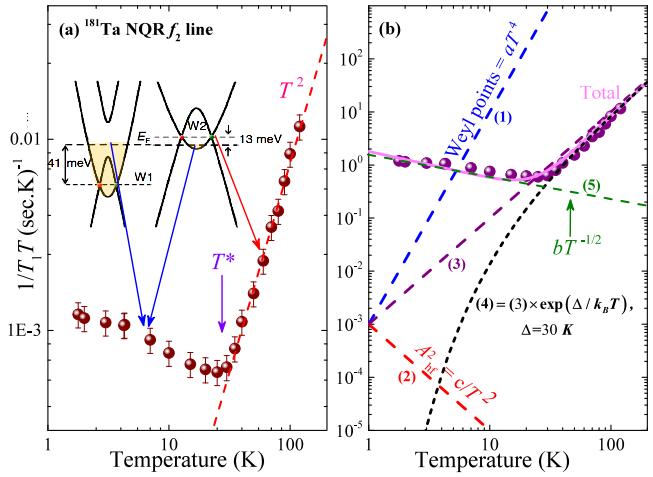

FIG. 3. (Color Online) (a) The temperature dependence of $1/T_1T$ of TaP along with the schematics of the band structure. At $T^* \approx 30$ K, the relaxation process crosses over between two different regimes. (b) Schematic illustration of Eq. (5): Curves (1), (2) and (3) are expected temperature dependence from the second term (Weyl nodes) not including the exponent, while curve (4) includes the exponent. The $T^{-1/2}$ dependence associated with the conventional bands is depicted by curve (5). The magenta curve is the total relaxation behavior expected from Eq. (5) and matches the experimental results.

and A_q is the q-dependent hyperfine coupling constant. Presently, a proper microscopic theory to accurately calculate $\chi(q,\omega)$ for multi-band systems is lacking. Consequently, we have evaluated a theoretical estimate for $1/T_1T$ based on non-interacting itinerant electrons approximation, using standard DFT. In the band structure of TaP, besides the normal bands, two types of Weyl points appear. The first set of Weyl points, termed W1 and located in the $k_z = 0$ plane, and lie $\sim$40 meV below E_F. The second set of Weyl points, W2, which lie nearly in the $k_z = \pi/c$ plane (c is the lattice parameter along z) are $\sim$13 meV above E_F.[12] This feature is shown schematically in the insert of Fig. 3(a) (see details in Supplement). Based on this band structure, one can easily imagine that the conventional Korringa process is valid for very low temperatures, with the upper bound limited by the energy of W2. Upon further increasing the temperature, excitations at the Weyl node W2 should become progressively dominant. Then, $1/T_1T$ may be phenomenologically expressed in a two-channel relaxation model by

$$\frac{1}{T_1T} = \frac{\pi k_B}{h}\left(A_p^{hf}\right)^2 N_p(E)^2 + \alpha\left[\left(A_w^{hf}\right)^2 \int \left\langle \frac{N_W(E)^2}{N_0^2} \right\rangle f(E)\{1-f(E)\}dE\right] \cdot exp\left(\frac{-\Delta E}{k_B T}\right) \quad (5)$$

where, the first term corresponds to excitations associated with parabolic bands ($E \propto k^2$) via the conventional Korringa process[27] with the hyperfine coupling constant A_p^{hf}. The second term is characteristic to the excitations of the Weyl nodes and linear bands ($E \propto k$) with A_w^{hf}. Herein, we have ignored the q dependence. α is the scaling factor. The term $N_w(E) = N_0 E/[E^2 - \Delta(\theta,\phi)]^{1/2}$ depends on the nodal structure and $f(E)$ is the Fermi distribution function. Because of the gap (ΔE) between W2 and E_F, we include an activation term, $exp(\Delta E/k_BT)$ in the second process. In general, for the point nodal case, we know $\Delta(\theta,\phi) = \Delta_0 sin\theta$, and $N(E) \propto E^2$; accordingly $1/T_1T \propto T^4$, which was observed experimentally for a point node superconductor.[28] Recently, anomalous hyperfine coupling due to orbital magnetism in the Weyl node has been predicted theoretically,[20] where the orbital contribution to A_w^{hf} has a $1/T$ dependence. Then, the second term of Eq. (5) becomes $T^2 exp(-\Delta E/k_BT)$. For the first term ($T < 30$ K), experimental data shows a $T^{-1/2}$ temperature dependence, despite the temperature independence of the Korringa process. The origin of this is not clear but we may speculate that correlation among excited quasiparticles may affect it. Setting $\Delta E/k_B \approx T^*$ (30 K), the expected temperature dependence is obtained by summing up the above contributions. As schematically shown in Fig 3. (b), choosing $\alpha = 10^{-3}$, Eq. (5) is in fairly good agreement with the experiment. In particular, we clearly see a T^2 dependence for $T > T^*$ which we believe to be the manifestation of Weyl fermion excitations near the Weyl points in TaP.

In conclusion, we have reported the observation of a complete set of ^{181}Ta NQR lines in Weyl semimetal TaP. All observed NQR lines are consistently assigned to the transitions between m- and $(m+1)$- states ($m = \pm 5/2$, $\pm 3/2$ and $\pm 1/2$). From our measurements, we obtain an asymmetry parameter $\eta = 0.423$ and a quadrupole coupling constant of $\nu_Q = 19.250$ MHz. These findings are in good agreement with DFT calculations which provide $\eta = 0.33$ and $\nu_Q = 20.057$ MHz. The low energy excitations as a function of temperature were probed through the Ta spin lattice relaxation rate ($1/T_1T$) which shows a pronounced T^2 behavior above $T^* = 30$ K and a $T^{-1/2}$ behavior below T^*. The relaxation process below T^* is mostly related to the conventional density of states ($N(E) \propto \sqrt{E}$) which yields an almost constant density of states at E_F (Korringa process). However, we have to postulate correlation effects as an origin for the $T^{-1/2}$ behavior below T^*. For $T > T^*$, by taking into account temperature dependent orbital hyperfine coupling and activation-type relaxation processes to the W2 points, we were able to explain the T^2 behavior in a convincing way. For the unique case of the Ta-based WSM, we have shown that the NQR method is a direct local probe for low energy Weyl fermion excitations in the bulk. This is rather important because such excitations are one of the main ingredients for the unconventional electrons trans-

port found in these new materials. It would be interesting to take a deeper look into other conventional bulk probes such as thermo-power to explore signatures of Weyl fermions, and to extend the NQR study to other Ta-based Weyl- and Dirac- semi metals.

Acknowledgement We thank B. Dóra for discussions and critical reading of the manuscript. Discussions with H. Harima, K. Kanoda, M. Majumder and E. Hassinger are also appreciated. T. K., Y. K. and H.T. appreciate the financial support from JSPS KAKENHI Grants (Nos.15K21732 and 15H05885).

* Michael.Baenitz@cpfs.mpg.de

[1] A. H. Castro Neto, F. Guinea, N. M. R. Peres, K. Novoselov, and A. Geim, Rev. Mod. Phys. **81**, 109 (2009).
[2] C. L. Kane and E. J. Mele, Phys. Rev. Lett. **95**, 146802 (2005).
[3] B. A. Bernevig, T. L. Hughes, and S. C. Zhang, Science **314**, 1757 (2006).
[4] M. Z. Hasan and C. L. Kane, Rev. Mod. Phys. **82**, 3405 (2010).
[5] T. O. Wehling, A. M. Black-Schaffer, and A. V. Balatsky, Advances in Phys. **63**, 1 (2014).
[6] S. M. Young, S. Zaheer, J. C. Y. Teo, C. L. Kane, E. J. Mele, and A. M. Rappe, Phys. Rev. Lett. **108**, 140405 (2012).
[7] Z. Wang, H. Weng, Q. Wu, X. Dai, and Z. Fang, Phys. Rev. B **88**, 125427 (2013).
[8] H. Weng, C. Fang, Z. Fang, B. A. Bernevig, and X. Dai, Phys. Rev. X **5**, 011029 (2015).
[9] C. Shekhar, A. K. Nayak, Y. Sun, M. Schmidt, M. Nicklas, I. Leermakers, U. Zeitler, Y. Skourski, J. Wosnitza, Z. Liu, Y. Chen, W. Schnelle, H. Borrmann, Y. Grin, C. Felser, and B. Yan, Nature Physics **11**, 645+ (2015).
[10] Y. Sun, S.-C. Wu, and B. Yan, Phys. Rev. B **92**, 115428 (2015).
[11] S.-Y. Xu, I. Belopolski, D. S. Sanchez, C. Zhang, G. Chang, C. Guo, G. Bian, Z. Yuan, H. Lu, T.-R. Chang, P. P. Shibayev, M. L. Prokopovych, N. Alidoust, H. Zheng, C.-C. Lee, S.-M. Huang, R. Sankar, F. Chou, C.-H. Hsu, H.-T. Jeng, A. Bansil, T. Neupert, V. N. Strocov, H. Lin, S. Jia, and M. Z. Hasan, Science Advances **1** (2015), 10.1126/sciadv.1501092.
[12] F. Arnold, C. Shekhar, S.-C. Wu, Y. Sun, R. D. dos Reis, N. Kumar, M. Naumann, M. O. Ajeesh, M. Schmidt, A. G. Grushin, J. H. Bardarson, M. Baenitz, D. Sokolov, H. Borrmann, M. Nicklas, C. Felser, E. Hassinger, and B. Yan, Nature Comm. **7** (2016), 10.1038/ncomms11615.
[13] N. Curro, *"Quadruplole NMR of superconductors" in Encyclopedia of Magnetic Resonance* (John Wiley & Sons, Ltd., 2011).
[14] N. J. Curro, Reports on Progress in Physics **72**, 026502 (2009).
[15] R. E. Walstedt, *The NMR Probe of High-T_c Materials*, Springer Tracts in Modern Physics, Vol. 228 (Springer-Verlag Berlin Heidelberg, 2008).
[16] Y. Kuramoto and Y. Kitaoka, *Dynamics of heavy electrons* (Oxford University Press INC. New York, 2000).
[17] G. Aeppli and Z. Fisk, Comments Condens. Matter Phys. **16**, 155 (1992); P. Riseborough, Adv. Phys. **49**, 257 (2000).
[18] T. Caldwell, A. P. Reyes, W. G. Moulton, P. L. Kuhns, M. J. R. Hoch, P. Schlottmann, and Z. Fisk, Phys. Rev. B **75**, 075106 (2007).
[19] E. M. Brüning, M. Brando, M. Baenitz, A. Bentien, A. M. Strydom, R. E. Walstedt, and F. Steglich, Phys. Rev. B **82**, 125115 (2010).
[20] Z. Okvátovity, F. Simon, and B. Dóra, ArXiv e-prints (2016), arXiv:1609.03370 [cond-mat.mes-hall].
[21] V. F. Mitrović, E. E. Sigmund, and W. P. Halperin, Phys. Rev. B **64**, 024520 (2001).
[22] J. Chepin and J. H. Ross, J. Phys.: Condens. Matter **3**, 8103 (1991).
[23] A. Abragam, *The Principle of Nuclear Magnetism* (Cladendon, Oxford, 1961); C. P. Slichter, *Principles of Magnetic Resonance* (Springer, New York, 1989).
[24] K. Koepernik and H. Eschrig, Phys. Rev. B **59**, 1743 (1999).
[25] J. P. Perdew and Y. Wang, Phys. Rev. B **45**, 13244 (1992).
[26] K. Koch, K. Koepernik, D. V. Neck, H. Rosner, and S. Cottenier, Phys. Rev. A **81**, 032507 (2010).
[27] J. Korringa, Physica **16**, 601 (1950).
[28] K. Katayama, S. Kawasaki, M. Nishiyama, H. Sugawara, D. Kikuchi, H. Sato, and G. qing Zheng, Journal of the Physical Society of Japan **76**, 023701 (2007).

Supplemental Material

TEMPERATURE DEPENDENCE OF ν_{Q} AND η

The temperature dependence of the quadrupole frequency $\nu_{\mathrm{Q}}(T)$ generally decreases with increasing temperature (Fig. S1) which is correlated to the lattice expansion. Owing to the fact that the origin of the EFG is the non-spherical distribution of surrounding point charges it may be easy to understand the thermally activated anharmonic phonon vibrations. This mechanism may be applicable to the case where onsite electric contribution to the EFG is negligibly small, and using the characteristic phonon frequency ν_{L}, $\nu_{\mathrm{Q}}(T)$ is expressed as

$$\nu_Q(T) = \nu_Q(0) \cdot \left(1 - \frac{\lambda h \nu_L}{k_B} \rho(T)\right) \qquad \text{(S1)}$$

where, $\rho(T)$ is the temperature dependent phonon distribution function given by $\rho(T) = \coth(h\nu_L/2k_BT)/2$ and λ is a lattice structure dependent parameter. Al-

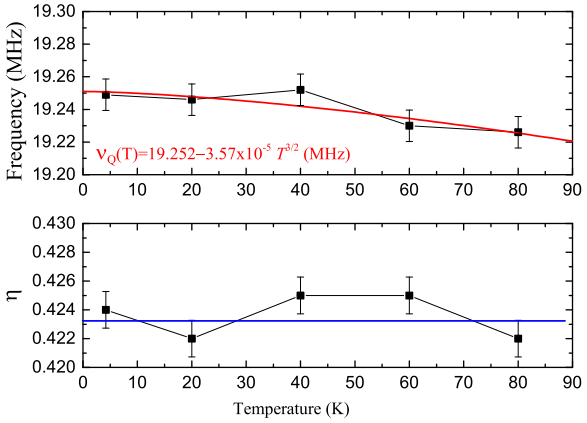

FIG. S1. Temperature dependence of ν_Q and η in TaP.

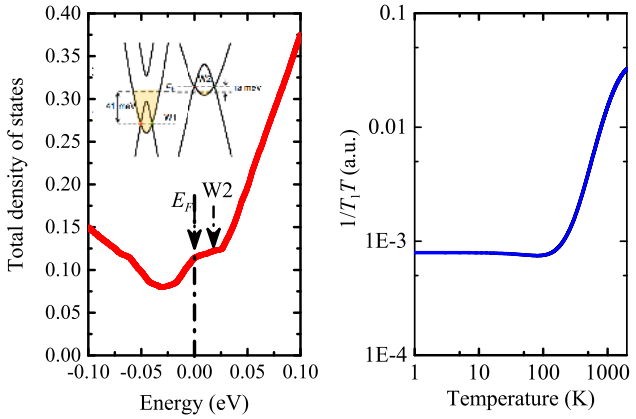

FIG. S2. (Left) Electronic density of states. The E_F (=8.257 eV) is shifted to zero. The positions of W1 and W2 Weyl points are illustrated in the inset. The W2 Weyl points are very close to E_F (Right) The temperature dependence of $1/T_1T$ (normalized to the experimental value at 2 K) on a logarithmic scale.

though Eq. (S1) has been applied successfully to insulating Cu_2O, the origin of the EFG in the present case is due to the onsite electric contribution related directly to the symmetry of the electronic wave function of the bands at the nucler site. In such a case, there is no analytical expression for $\nu_Q(T)$. Therefore, we adopt an empirical form for conventional non-cubic metals,[S1]

$$\nu_Q(T) = \nu_Q(0) \cdot (1 - A \cdot T^{3/2}), A > 0 \qquad \text{(S2)}$$

where there exists a correlation between the magnitude of $\nu_Q(0)$ and the strength of the EFG's temperature variation, quantified by the coefficient A. A least-squares fit of the data above 60K to Eq. (S2) yields the following values: ν_Q = 19.252 MHz, $A = 3.57\times10^{-5}$ K$^{-3/2}$.

CALCULATION OF $1/T_1T$ FROM NON-INTERACTING BAND STRUCTURE IN TAP

We have performed $ab-initio$ density functional theory calculations for the band structure of the TaP using the Vienna ab-initio simulation package (VASP)[S2] employing the modified Becke-Johnson (MBJ) potential[S3] for the exchange-correlation functions. Then we projected the DFT Bloch wave functions into the maximum localized Wannier functions by the Wannier90 package.[S4] Based on the tight-binding Wannier Hamiltonian, we interpolate the density of states by a dense k-grid of 400 × 400 × 400 in the first Brillouin zone. Calculated $N(E)$ are shown in Fig. S2 (left). The nuclear spin-lattice relaxation rate for non-interacting electrons are calculated by the following formula[S4, S5]:

$$\frac{1}{T_1} = \frac{\pi}{\hbar}(\gamma_e\gamma_n\hbar^2)^2(A^\perp)\int_{-\infty}^{\infty} dE D_+(E)f(E) \cdot \int_{-\infty}^{\infty} dE' D_-(E')[1-f(E')]\delta(E-E') \qquad \text{(S3)}$$

where, $A^\perp$ is the hyperfine coupling constant; γ_e, γ_n are the electronic and nuclear gyromagnetic ratios, respectively. The electronic density of states for spin up and spin down electrons is simply evaluated via Zeeman splitting $D_\pm = E(E \mp E_z/2)/2$ (we take $E_z = 0$ here to estimate the zero field case). $f(E)$ is the Fermi-Dirac distribution to include temperature dependent behavior and $\delta(E - E')$ is the delta function. As we are mainly interested in the temperature-dependence of T_1, the prefactors before the integral make no difference in the general trend. Thus, we normalized arbitrarily the calculated values to the experimental value at 2K, which is shown in Fig. S2 (right). Although the general feature is similar to the experiment, it should be noted that the energy scale of the point where $1/T_1T$ starts increase is roughly one order of magnitude larger than the experimental value and the W2 energy. So, we can conclude that the increase of $1/T_1T$ here is just due to the influence of other bands and not related to the excitations around Weyl points. One of the possible origins of this discrepancy is the lack of an adequate account of electron-electron interactions in theory.

* Michael.Baenitz@cpfs.mpg.de

[S1] J. Christiansen, P. Heubes, R. Keitel, W. Klinger, W. Loeffler,W. Sandner, and W. Witthuhn, Z. Phys. B: Condens. Matter **24**,177 (1976).
[S2] J. Chepin and J. H. Ross, J. Phys.: Condens. Matter **3**, 8103 (1991).
[S3] J. P. Perdew, K. Burke, and M. Ernzerhof, Phys.Rev.Lett. **77**, 3865 (1996).

[S4] A. A. Mosto, J. R. Yates, Y. S. Lee, I. Souza, D. Vanderbilt, and N. Marzari, Comput. Phys. Commun. **178**, 685 (2008).

[S5] Hirata Michihiro, Kyohei Ishikawa, Kazuya Miyagawa, Masafumi Tamura, Claude Berthier, Denis Basko, Akito Kobayashi, Genki Matsuno, and Kazushi Kanoda, Nature Communications **7** (2016).